Materials Letters 65 (2011) 215–218

Contents lists available at ScienceDirect

Materials Letters

journal homepage: www.elsevier.com/locate/matlet

A facile route to prepare PdPt alloys for ethanol electro-oxidation in alkaline electrolyte

Sheng-Chieh Lin, Jing-Yu Chen, Yi-Fan Hsieh, Pu-Wei Wu *

Department of Materials Science and Engineering, National Chiao Tung University, Hsin-Chu 300, Taiwan

ARTICLE INFO

Article history:
Received 5 June 2010
Accepted 2 October 2010
Available online 8 October 2010

Keywords:
Catalyst
Displacement reaction
PdPt
Ethanol electro-oxidation

ABSTRACT

We adopted a displacement reaction in acidic solution that enabled the spontaneous reduction of Pd and Pt cations in conjunction with corrosive dissolution of Ni. The composition for the PdPt was adjusted by varying the concentration of Pd and Pt cations. From SEM images and XRD patterns, the PdPt formed an fcc alloy uniformly deposited on the Ni substrate. Electro-oxidation of ethanol was conducted in alkaline electrolyte for samples of Pd, Pt, and PdPt alloys. In cyclic voltammetric profiles, the $Pd_{77}Pt_{23}$ revealed the highest electrocatalytic ability in both apparent current and mass activity, followed by $Pd_{87}Pt_{13}$, Pd, and Pt. Similar behaviors were observed in life time measurements in which stable performances for ethanol electro-oxidation were obtained.

1. Introduction

Fuel cells have attracted considerable attention recently as clean power sources because of their better conversion efficiency and reduced emission over conventional alternatives [1,2]. In particular, the direct ethanol fuel cell is of significant interest since the ethanol not only contains sufficient energy density but also can be produced from sugar fermentation [3,4]. In an acidic environment, the electro-oxidation of ethanol is rather slow which is caused by the poor ability of Pt to break C–C bonds. Alloying the Pt with other constituents produces limited progress as only selective corrosion-resistant elements such as Ru and Sn can be employed [5,6]. On the other hand, the electro-oxidation of ethanol in an alkaline electrolyte is more feasible because many metals can be explored [7,8]. In addition, the oxygen reduction reaction is much facile in an alkaline medium so the overall polarization loss for the fuel cell system can be largely reduced.

In alkaline electrolyte, the Ni is widely employed as the electrode support for its chemical stability, and the Pd and its alloys are often used as electrocatalysts. For example, Lu et al. adopted an electrodeposition technique to fabricate Pd_xPt_{1-x} and reported their impressive catalytic abilities [9]. In addition, Bagchi and Bhattacharya demonstrated that the PdRu deposited on a Ni foil revealed notable catalytic stability with reduced poisoning effect [10]. A similar catalytic stability was also found in the PdAu [11]. Because the Ni is unstable in acidic solution, a simpler approach to fabricate electrocatalysts is to initiate a displacement reaction that allows corrosive dissolution of Ni and spontaneous reduction of cations from the solution. The displacement reaction occurs in binary systems with constituents revealing distinct values of redox potentials. For example, the synthesis for PtPd and AuPd has been demonstrated for ethanol electro-oxidation [12,13]. In general, the displacement reaction is known for fabricating core–shell nanoparticles with tailored surface compositions. But typical catalyst fabrication schemes in literature involve direct chemical or hydrogen reduction instead, which are much simpler to operate. This displacement reaction can also be applied to form binary or tertiary alloy nanoparticles. For example, Bambagioni et al. successfully deposited the Pd onto NiZn nanoparticles and reported notable ethanol oxidation behaviors [14].

Since both Pt and Pd reveal distinct redox potentials, in this work we demonstrate that a PdPt alloy can be easily prepared via the displacement route. The same scheme can be employed to prepare electrocatalysts with multiple constituents in a simple step provided that their respective cation concentrations are carefully controlled.

2. Experimental

Spontaneous deposition of PdPt alloy was carried out on a Si wafer (4 cm^2) coated with Ni via an electroless deposition. The Si wafer was predeposited with SiO_2 (500 nm), TaN (20 nm), and Cu (60 nm), followed by an activation treatment for 10 s in 50 ml solution containing 5 mM $PdCl_2$ and 7 mM HCl. After Pd seeding, the sample was submerged in a plating bath which included 20 g/L of $NiSO_4$–$6H_2O$ as the metal source and 25 g/L of NaH_2PO_2 as the reducing agent. In addition, 2 ppm of $Pb(NO_3)_2$ was added as the stabilizing agent and 0.5 M of NaOH was used to adjust the pH to 5.5. The electroless process was maintained at 70 °C for 1 h to obtain a uniform Ni–P coating. Next, the Ni–P coated sample was immersed in 20 ml solution containing 5 mM of $PdCl_2$ and H_2PtCl_6. Their molar ratio was adjusted at 1:0, 2:1, 5:1, and 0:1 to form

* Corresponding author. Tel.: +886 3 5131227; fax: +886 3 5724727.
E-mail address: ppwu@mail.nctu.edu.tw (P.-W. Wu).

0167-577X/$ – see front matter © 2010 Elsevier B.V. All rights reserved.
doi:10.1016/j.matlet.2010.10.006

deposits of Pd, Pd_xPt_{1-x}, and Pt via the displacement reaction at 25 °C for 2 min. The samples obtained were designated as Pd, 2PdPt, 5PdPt, and Pt, respectively.

Morphology and thickness for the PdPt deposit were observed by a FE-SEM (JSM 6500). Composition determination was conducted by ICP-MS (Perkin Elmer, SCIEX ELAN 5000). Phase and crystallinity were identified by X-ray diffractometer (Max Science M18XHF). Electrochemical analysis was performed by cyclic voltammetry (CV) in 1 M KOH and 1 M C_2H_5OH using a Solartron SI 1287 for −1 to −0.3 V at 50 mV/s. A three-electrode setup was adopted in which a Pt foil (5.7 cm^2), Ag/AgCl, and PdPt/Ni (1 cm^2) were used as the counter, reference, and working electrode, respectively. Life time behaviors were obtained from chronoamperometric curves at −0.3 V for 60 min. Both the CV and life time measurements were conducted at 25 °C.

3. Results and discussion

Fig. 1 provides the SEM images for the Pd, Pt, 2PdPt, and 5PdPt in planar and cross-sectional views. As shown in Fig. 1a, an overcoat of Pd was uniformly deposited on the Ni substrate with some irregular protrusions in sizes of 50–150 nm. From the cross-sectional view, the thickness for the Pd was 43.4 nm. Notably, the cluster boundaries for the Ni substrate were still visible. Shown in Fig. 1b is the image for the Pt which existed in c.a. 75 nm particles with significant coalescence. Interestingly, the Pt coverage was not complete as the Ni substrate underneath was still discernible. The cross-sectional image also demonstrated a similar microstructure of nodular Pt connected to each others. Fig. 1c exhibits the image for the 2PdPt sample where a wider size distribution in 15–100 nm was observed and most of them revealed a coalescence behavior. The cross-sectional view confirmed its height of 40 nm. Shown in Fig. 1d is the image for 5PdPt. Its morphology was similar to that of Fig. 1a in which an overcoat was formed with considerable surface roughness. Again, the cross-sectional image indicated a height of 37.5 nm.

In an acidic electrolyte, the displacement reaction of Pd and Pt on the Ni substrate involves an oxidative dissolution of Ni in conjunction with spontaneous reduction of Pd^{2+} and $PtCl_6^{2-}$ from the electrolyte. The associated reaction steps and redox values are listed below:

$$PtCl_6^{2-} + Ni = PtCl_4^{2-} + 2Cl^- + Ni^{2+}, E = 0.99V \quad (1)$$

$$PtCl_4^{2-} + Ni = Pt + 4Cl^- + Ni^{2+}, \quad E = 1.02V \quad (2)$$

$$Pd^{2+} + Ni = Pd + Ni^{2+}, \quad E = 1.21V. \quad (3)$$

The pH value for the $PdCl_2$ and H_2PtCl_6 solution was 2.03 and 1.84, respectively and these values remained relatively unchanged during the displacement reaction. Therefore, the Pd was expected to deposit faster than Pt despite the Pt revealed a lower overall redox potential. It is because the Pt reduction entailed two stages of two-electron reaction while the Pd only required a single step to complete. Results from the ICP-MS are provided in Table 1, which confirmed our premise. In addition, the SEM images in Fig. 1 also indicated an accelerated deposition of Pd over Pt. The $Pb(NO_3)_2$ was added as a stabilizer in the electroless Ni plating solution. However, it was not used in the displacement bath for Pd and Pt deposition. In EDX analysis on the electroless-derived Ni, we did not observe any Pb signal. According to Yin et al., the Pb was found in the Ni deposit by XPS when its concentration was above 10 ppm [15]. In our case, we only used 2 ppm of $Pb(NO_3)_2$ so its residual amount in the Ni deposit was likely to be reduced and its effect on the ethanol electro-oxidation was rather negligible.

Fig. 2 presents the XRD spectra for the Ni, Pd, Pt, 2PdPt, and 5PdPt, respectively. As shown, the Ni revealed a nanocrystalline nature with a broad peak at 44.5° identified as (111). Since the NaH_2PO_2 was used as the reducer, the Ni deposit contained 15 at.% of P that lead to the nanocrystalline state. In contrast, both Pd and Pt demonstrated an fcc

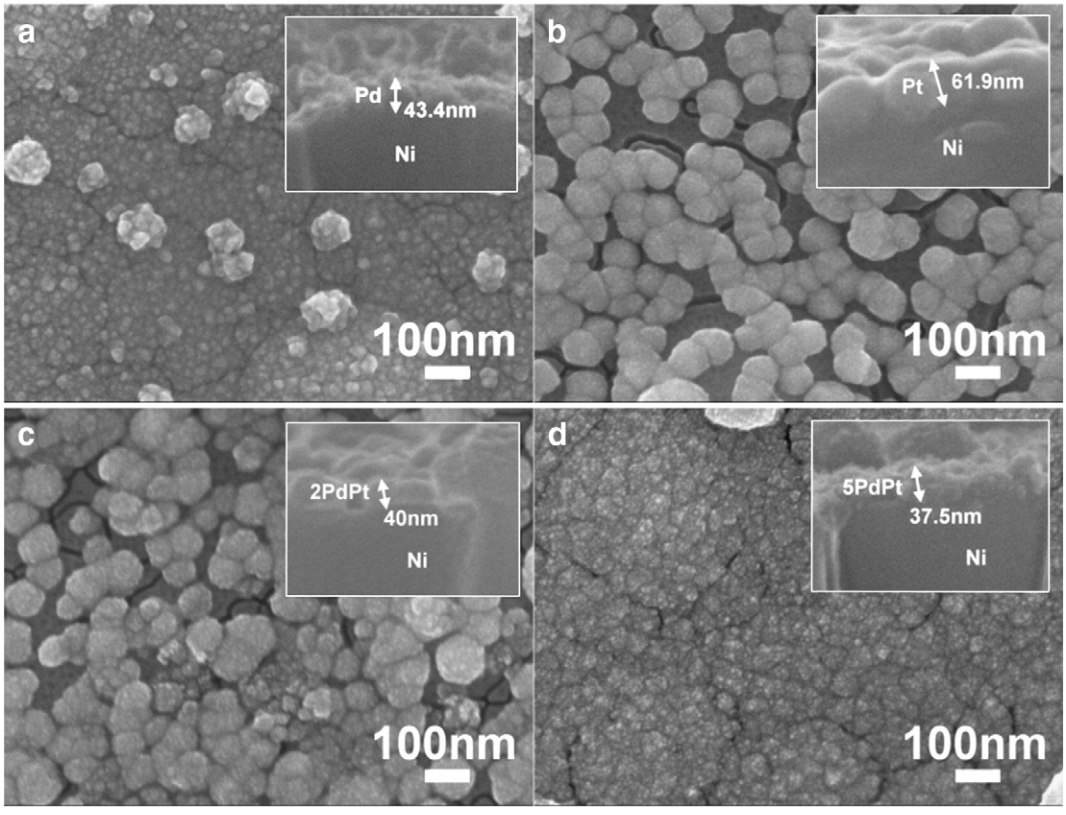

Fig. 1. SEM images in planar and cross-sectional views for the (a) Pd, (b) Pt, (c) 2PdPt, and (d) 5PdPt, respectively.

Table 1
Materials properties for the Pd, Pt, 2PdPt, and 5PdPt.

Sample	Pd loading ($\mu g/cm^2$)	Pt loading ($\mu g/cm^2$)	Total loading ($\mu g/cm^2$)	Pd/Pt atomic ratio	XRD (111) (2θ)	Lattice parameter (Å)	Crystallite size (nm)
Pt	0.00	37.34	37.34	0/100	39.70	3.929	5.4
2PdPt	48.26	26.24	74.50	77/23	39.96	3.905	8.4
5PdPt	56.54	15	71.88	87/13	39.98	3.903	8.2
Pd	72.49	0.00	72.49	100/0	40.06	3.895	6.7

phase with relevant planes properly indexed. In addition, their peak position and relative intensity agreed with their respective JCPDS file (Pd: JCPDS-46-1043; Pt: JCPDS-04-0802). Notably, the Pd (200) and Pt (200) signals were mixed with the Ni (111) that rendered a broad diffraction signal. Similar diffraction patterns were observed for the 2PdPt and 5PdPt. Since both Pd (1.37 Å) and Pt (1.39 Å) adopt an fcc structure, their alloys are expected to form a solid solution with the resulting lattice parameter slightly modified by the Pd/Pt ratio. Hence, the Pd lattice experiences a slight expansion when the Pt is alloyed because the latter has a relatively larger atomic radius. Table 1 lists the lattice parameter from the (111) peak and estimated crystallite size from Scherrer equation. The minor variation in the lattice parameter was expected and consistent with earlier reports by Wang et al. and Xiao et al. [16,17].

Fig. 3 demonstrates the CV profiles in apparent current density and mass activity for ethanol electro-oxidation for Pt, Pd, 2PdPt, and 5PdPt, respectively. From literature, the electro-oxidation of ethanol on the Pd surface takes places via the adsorption of ethanol followed by reaction with hydroxyl ions, resulting in the formation of CH_3COOH [18].

$$Pd + C_2H_5OH = Pd - (C_2H_5OH)_{ads} \quad (4)$$

$$Pd - (C_2H_5OH)_{ads} + 3OH^- = Pd - (CH_3CO)_{ads} + 3H_2O + 3e \quad (5)$$

$$Pd + OH^- = Pd - (OH)_{ads} + e \quad (6)$$

$$Pd - (CH_3CO)_{ads} + Pd - (OH)_{ads} = 2Pd + CH_3COOH \quad (7)$$

Previously, it was reported that the Pt was unable to electro-oxidize ethanol efficiently as compared to Pd [19]. This behavior was confirmed in the CV profiles where a significantly reduced current was observed for the Pt. In contrast, the Pd revealed notable anodic and cathodic peaks which were consistent with what were reported earlier [20]. The anodic peak was attributed to reaction (5) in the formation of adsorbed Pd-(CH_3CO). Once the anodizing potential was above −0.2 V, the oxidation of Pd to PdO was occurring which deactivated the Pd from reactions (4) and (5), resulting in a decreasing current. During the cathodic scan, the PdO was reduced to Pd, allowing the adsorption of OH^- via reaction (6). Afterward, the adsorbed OH reacted with the adsorbed CH_3CO, completing the oxidation of ethanol to acetic acid. From the CV curves, the Pt, 2PdPt, 5PdPt, and Pd revealed the onset potential of −0.7, −0.72, −0.72, and −0.7 V, respectively. These values were similar to what have been reported in literature. For example, in the study of Pd_xPt_{1-x} on Ti, Lu et al. reported the onset potentials of −0.63 to −0.74 V [9]. Among these samples, the PdPt alloys

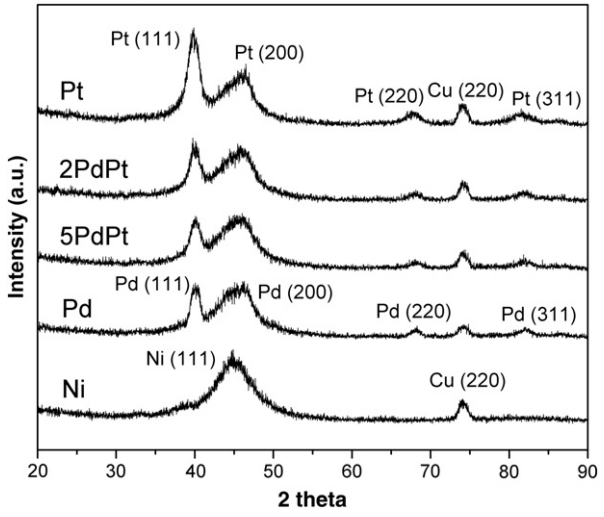

Fig. 2. XRD spectra for the Ni, Pd, Pt, 2PdPt, and 5PdPt, respectively.

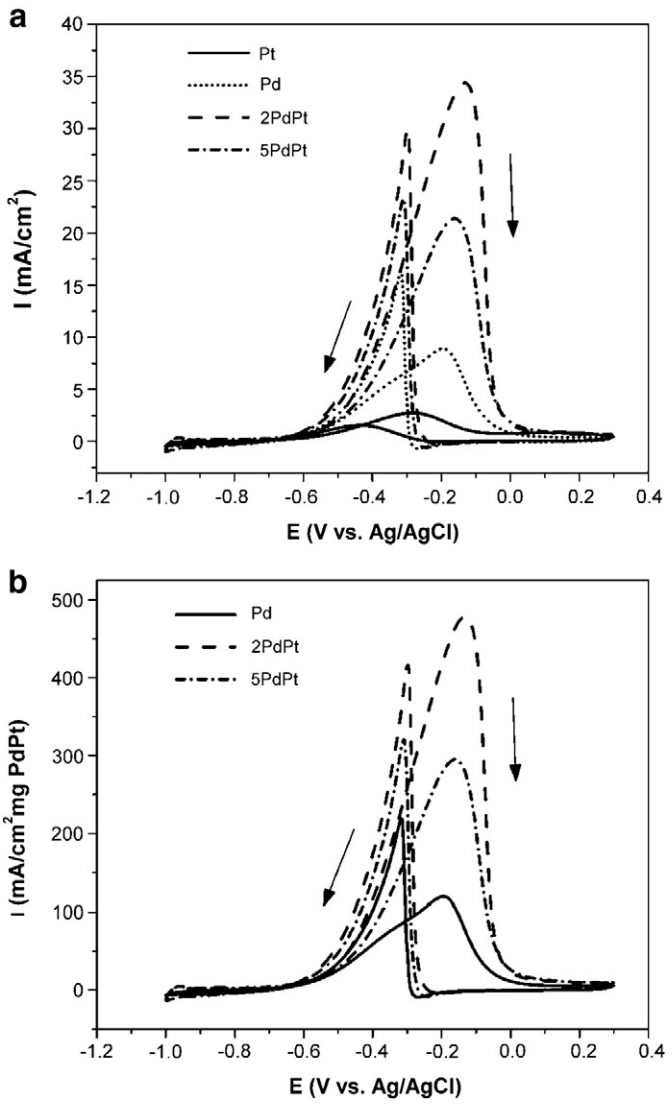

Fig. 3. CV profiles in (a) apparent current density and (b) mass activity for the Pt, Pd, 2PdPt, and 5PdPt, respectively.

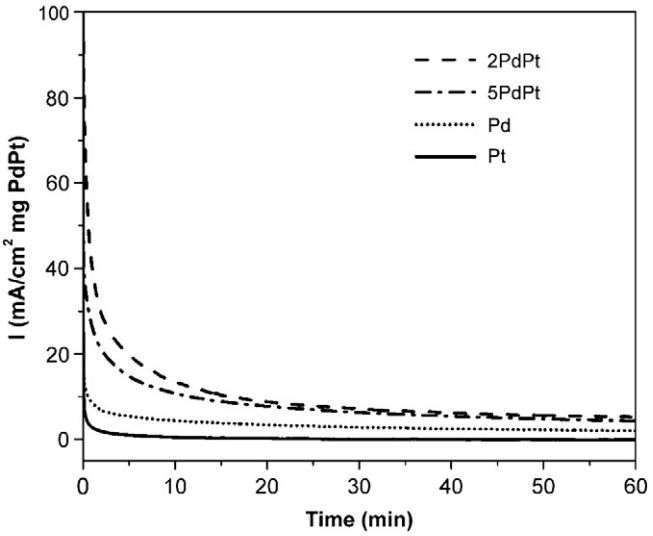

Fig. 4. Chronoamperometric curves for Pt, Pd, 2PdPt, and 5PdPt, respectively.

exhibited considerable improvements over that of Pd. In particular, the sample of 2PdPt ($Pd_{77}Pt_{23}$) delivered the highest oxidation current. Because their SEM surface morphologies were similar, the improvement in the catalytic ability was attributed primarily to the variation of surface state after alloying. Similar behaviors of enhancement in PdPt alloys were recently demonstrated by Lu et al. [9]. We rationalized that the observed catalytic enhancement was possibly due to the electronic effect in which the d-band center of Pd was raised by the presence of Pt nearby. This promoted the absorption of OH^- that facilitated the oxidation of adsorbed CH_3CO. Alternative, the Pt was able to adsorb OH^- directly which promoted the oxidation of adsorbed CH_3CO on the Pd (bifunctional model). In the mass activity presented in Fig. 3b, we observed similar trends that the 2PdPt revealed the highest mass activity (>478 mA/cm^2 mg PdPt) and lowest onset potential.

Fig. 4 provides the life time performance at −0.3 V for 60 min. As shown, the current experienced a rapid deterioration with increasing time but became stabilized after 30 min. It is believed that at this stage the adsorption and desorption of intermediates reached a steady state that allowed the electro-oxidation of ethanol at a fixed rate. As expected, the sample of 2PdPt delivered the best performance followed by 5PdPt, Pd, and Pt. This trend was consistent with what we observed in CV profiles shown in Fig. 3.

4. Conclusions

We successfully demonstrated the fabrication of PdPt alloys on a Ni substrate using a displacement reaction in acidic solution. Both SEM images and XRD patterns confirmed the morphology and crystalline state for the PdPt deposit. For the ethanol electro-oxidation in alkaline solution, the sample of 2PdPt ($Pd_{77}Pd_{23}$) revealed the highest electro-catalytic ability in both CV and life time measurements followed by 5PdPt ($Pd_{87}Pd_{13}$), Pd, and Pt.

Acknowledgement

Financial supports from the National Science Council of Taiwan (98-2221-E-009-040-MY2) are greatly appreciated.

References

[1] Steele CH, Heinzel A. Nature 2001;414:345–52.
[2] Zhang XY, Li D, Dong DH, Wang HT, Webley PA. Mater Lett 2010;64:1169–72.
[3] Song SQ, Tsiakaras P. Appl Catal B 2006;63:187–93.
[4] Lamy C, Lima A, LeRhun V, Delime F, Coutanceau C, Léger JM. J Power Sources 2002;105:283–96.
[5] Jiang LH, Sun GQ, Wang SL, Wang GX, Xin Q, Zhou ZH, et al. Electrochem Commun 2005;7:663–8.
[6] Liu HS, Song CJ, Zhang L, Zhang JJ, Wang HJ, Wilkinson DP. J Power Sources 2006;155:95–110.
[7] Antolini E, Gonzalez ER. J Power Sources 2010;195:3431–50.
[8] Bianchini C, Shen PK. Chem Rev 2009;109:4183–206.
[9] Lu JL, Lu SF, Wang DL, Yang M, Liu ZL, Xu CW, et al. Electrochim Acta 2009;54:5486–91.
[10] Bagchi J, Bhattacharya SK. Trans Met Chem 2007;32:47–55.
[11] Nie M, Tang H, Wei Z, Jiang SP, Shen PK. Electrochem Commun 2007;9:2375–9.
[12] Zheng HT, Chen S, Shen PK. Electrochem Commun 2007;9:1563–6.
[13] Cheng F, Dai X, Wang H, Jiang SP, Zhang M, Xu C. Electrochim Acta 2010;55:2295–8.
[14] Bambagioni V, Bianchini C, Filippi J, Oberhauser W, Marchionni A, Vizza F, et al. ChemSusChem 2009;2:99–112.
[15] Yin X, Hong L, Chen BH. J Phys Chem B 2004;108:10919–29.
[16] Wang WM, Huang QH, Liu JY, Zou ZQ, Li AL, Yang H. Electrochem Commun 2008;10:1396–9.
[17] Xiao F, Zhao FQ, Mei DP, Mo ZR, Zeng BH. Biosens Bioelectron 2009;24:3481–6.
[18] Liu JP, Ye JQ, Xu CW, Jiang SP, Tong YX. Electrochem Commun 2007;9:2334–9.
[19] Liang ZX, Zhao TS, Xu JB, Zhu LD. Electrochim Acta 2009;54:2203–8.
[20] Xu CW, Cheng LQ, Shen PK, Liu YL. Electrochem Commun 2007;9:997–1001.